Engineering personalized neural tissue by combining induced pluripotent stem cells with fibrin scaffolds

Amy Montgomery, Alix Wong, Nicole Gabers, and Stephanie M. Willerth

2015

The final published version of this article can be found at:

http://dx.doi.org/10.1039/C4BM00299G

Cite this: DOI: 10.1039/x0xx00000x

Engineering personalized neural tissue by combining induced pluripotent stem cells with fibrin scaffolds

Amy Montgomery[a] Alix Wong[b], Nicole Gabers[c], and Stephanie M. Willerth[a,d]

Received 00th January 2012,
Accepted 00th January 2012

DOI: 10.1039/x0xx00000x

www.rsc.org/

[a] Department of Mechanical Engineering, University of Victoria
[b] Department of Biochemistry and Microbiology, University of Victoria
[c] Department of Biology, University of Victoria
[d] Division of Medical Science, University of Victoria

Induced pluripotent stem cells (iPSCs) are generated from adult somatic cells through the induction of key transcription factors that restore the ability to become any cell type found in the body. These cells are of interest for tissue engineering due to their potential for developing patient-specific therapies. As the technology for generating iPSCs advances, it is important to concurrently investigate protocols for the efficient differentiation of these cells to desired downstream phenotypes in combination with biomaterial scaffolds as a way of engineering neural tissue. For such applications, the generation of neurons within three dimensional fibrin scaffolds has been well characterized as a cell-delivery platform for murine embryonic stem cells (ESCs) but has not yet been applied to murine iPSCs. Given that iPSCs have been reported to differentiate less effectively than ESCs, a key objective of this investigation is to maximize the proportion of iPSC-derived neurons in fibrin through the choice of differentiation protocol. To this end, this study compares two EB-mediated protocols for generating neurons from murine iPSCs and ESCs: an 8-day 4-/4+ protocol using soluble retinoic acid in the last 4 days and a 6-day 2-/4+ protocol using soluble retinoic acid and the small molecule sonic hedgehog agonist purmorphamine in the last 4 days. EBs were then seeded in fibrin scaffolds for 14 days to allow further differentiation into neurons. EBs generated by the 2-/4+ protocol yielded a higher percentage of neurons compared to those from the 4-/4+ protocol for both iPSCs and ESCs. The results demonstrate the successful translation of the fibrin-based cell-delivery platform for use with murine iPSCs and furthermore that the proportion of neurons generated from murine iPSC-derived EBs seeded in fibrin can be maximized using the 2-/4+ differentiation protocol. Together, these findings validate the further exploration of 3D fibrin-based scaffolds as a method of delivering neuronal cells derived from iPSCs – an important step toward the development of iPSC-based tissue engineering strategies for spinal cord injury repair.

1 Introduction

Pluripotent stem cells have two key properties: immortality – the ability to continuously self-renew – and pluripotency – the ability to differentiate into all somatic cell types. Tissues are derived from these cells during early development. In 1981, murine embryonic stem cells (ESCs) were successfully isolated from the inner cell mass of mouse blastocycts [1, 2]. This discovery was followed by the establishment of human ESC lines derived from the inner cell mass of a blastocyst nearly two decades later [3]. More recently, it was discovered that somatic cells could be reverted to a stem cell state by the induction of certain genetic factors involved in regulating immortality and pluripotency [4-6]. These cells are known as induced pluripotent stem cells (iPSCs). Both ESCs and iPSCs are powerful tools for regenerative medicine as they have the potential to supplement or replace tissues that are adversely affected by disease or injury. Due to their derivation from adult somatic cells, iPSCs offer the further advantages that they avoid the controversial use of blastocysts and also make possible the generation of patient-specific tissues.

The field of iPSC generation is quickly evolving, making the cells increasingly more promising from a therapeutic standpoint. For instance, the first studies in 2007 reported less than 1% of transfected somatic cells becoming pluripotent stem cells [7] but a 2013 study achieved a near 100% efficiency through inhibition of a key protein implicated in blocking the transcription of transfected genes [8]. Progress is also being made to address safety concerns related to the use of retroviral vectors for the transfection of somatic cells for iPSC generation as they introduce the risk of insertional mutagenesis or may provoke an immune response. Methods of non-integrating transfection have been introduced, such as using high concentrations of plasmids for reprogramming somatic cells [9]. However, these methods have not yet demonstrated reprogramming efficiencies to match those of retroviral transfection. Another safety concern is related to the sustained proliferation of implanted cells. To address this, a protocol to evaluate non-tumor forming "safe" iPSC lines was developed for therapeutic applications [10, 11]. When this screening process is used, iPSCs show a lower risk of tumour formation compared to otherwise unscreened ESCs. Thus, as many laboratories continue to tackle these challenges associated with iPSC generation, it is critical that the biomaterials and tissue engineering field concurrently investigate the appropriate cell-delivery tools and downstream differentiation protocols for iPSC-

derived cells in order to incorporate the advancing iPSC technology effectively.

Studies suggest that while iPSCs follow the same transcriptional regulation as ESCs for neural differentiation [12], current differentiation protocols do not produce these cell types with the same efficiency in iPSCs [12, 13]. This difference may be due to the forced expression of reprogramming factors used to generate iPSCs that relies on artificial promoters, which can interfere with the natural expression of these factors during differentiation [13] or epigenetic factors which may predispose different iPSC cell lines to particular lineages [12]. Furthermore, the somatic cell type from which iPSCs are derived and choice of reprogramming factors affect the ability of the cells to differentiate into desired types [14]. However, despite the comparatively lower efficiency, these studies have shown successful differentiation of iPSCs into neural phenotypes including, neurons, astrocytes, and oligodendrocytes [11-14]. Thus, progress toward more efficient neural differentiation protocols represents an important step in the development of clinically relevant iPSC-based regenerative therapies for the diseases and disorders of the nervous system [15].

As early as the first studies in the 1980s, murine stem cells have been directed to differentiate *in vitro* through removal from media conditioned for maintenance of pluripotency and subsequent culture in suspension on non-adhesive plates. The result of this process is the formation of suspended cell aggregates called embryoid bodies (EBs) which contain multipotent progenitor cell types of all three germ layers [16]. One of the standard protocols for producing EBs containing neural progenitors was published in 1995 by Bain *et al.* [17] to include treatment with 500 nM retinoic acid (RA) during the last 4 days of an 8 day induction period, often referred to as the "4-/4+ protocol". This protocol was derived from previous work on teratocarcinoma lines and a growing body of evidence in the field of developmental biology that implicated this retinol derivative in the development of the brain and spinal cord [18, 19]. Based on these studies and others, RA has been well characterized as an important signalling factor in neural differentiation. However, some of the underlying mechanisms of RA-mediated patterning – in particular its action as a potential morphogen across a concentration gradient – are not fully understood. Experiments involving the exposure of cultured cells to RA are known to be complicated by the concentration-, stage-, or duration-dependent effects [19] and, as such, protocols for the differentiation of pluripotent stem cells which involve RA remain relevant avenues of investigation.

More recently, other factors emerged as potential targets for in vitro neural differentiation protocols. For instance, in the developing mammalian neural tube, ventrally expressed sonic hedgehog (Shh), dorsally expressed bone morphogenetic proteins (BMPs), and fibroblast growth factor (FGF) expressed at the posterior end of the neural tube, together with RA generated in the somites of the adjacent mesoderm, are all known to direct the patterning of the spinal cord [18]. In particular, Shh signalling plays a key role in neural development. In the developing vertebrate, Shh is expressed ventral to the neural tube and a gradient of signalling from ventral to dorsal is responsible for the patterning and specification of five ventral neural progenitor sub-types in a manner inversely proportional to the distance from this source [20]. The neural progenitor sub-types then differentiate into distinct neuronal sub-types, including commissural neurons, association neurons, motor neurons, and ventral interneurons [21]. This morphogenic effect can be replicated *in vitro*, as the differentiation of motor neuron and interneuron cell types which are found closer to the source of Shh in vivo requires a higher dose of Shh compared to the sensory neuron subtypes found dorsally [21].

The application of both RA and Shh during embryoid body formation in murine ESCs was investigated by Wichterle *et al.* [22], Miles *et al.* [23], Kothapalli and Kamm [24], Brown *et al.* [25], and in human ESCs by Li *et al.* [26], Stacpoole *et al.* [27], and Hu and Zhang [28], among others. Such studies have revealed the synergistic effects of these two factors. For example, Wichterle *et al.* reported that RA and Shh together increased the number of post mitotic neurons generated from mESC EBs, Shh alone did not appear to have an effect on neural induction [22]. Kothapalli and Kamm reported that the addition of Shh, either alone or with RA, to mESCs in 3D collagen matrices significantly improved neuronal differentiation relative to control cultures. However, it was also observed that neurite outgrowth was inhibited in the cultures with Shh and RA compared to those with RA alone [24].

It has also been found that the concentrations of RA and Shh can be tailored to achieve differentiation of ESCs into particular neuronal subtypes. For example, Kothapalli and Kamm found that the addition of RA alone to mESCs in 3D collagen matrices is optimal for dopaminergic neuron formation while the addition of RA and Shh to mESCs in 3 matrigel matrices is optimal for dopaminergic neuron formation [24]. Brown *et al.* reported that the specific neuronal subtype V2a interneurons can be generated from mESCs through exposure to low concentration of RA (10 nM) and mild Shh agonist whereas high RA concentration (up to 10 μM) and a high potency Shh agonist limit these results [25]. In applications presented by Stacpoole *et al.* as well as Hu and Zhang, hESCs are differentiated into spinal motor neurons by first exposing NPCs to RA to caudalize the cells, followed by the combination of RA and Shh (or Shh agonist) in the subsequent days to ventralize them [27, 28]. In the absence of Shh exposure, it was found that cells are not necessarily restricted to ventral fate [29].

Following the report of the small synthetic molecule purmorphamine activating the Shh signal transduction cascade [30], the substitution of purmorphamine for Shh was suggested [31]. A key advantage of the commercially produced synthetic molecule purmorphamine is its stability and affordability compared with Shh [32]. The first reported use of purmophamine in an EB-mediated protocol for the differentiation of neurons from murine ESCs was by Pellet et al. [33] in a 2011 study on the development of a cell-based assay for detection of botulinum neurotoxin. The method described is a modified version of the 4-/4+ differentiation protocol executed over a shorter 6-day period and involving treatment with 500 nM RA and 1 μM purmorphamine in the last 4 days of induction. This method, referred to as the "2-/4+ protocol" has been adopted by other studies that seek to differentiate pluripotent stem cells into neurons [34].

Given the impetus to produce viable cells in a relatively short amount of time, the truncated differentiation period of the 2-/4+ protocol is desirable, provided that it does not have a negative impact on the overall differentiation. It is not clear, however, which protocol is better suited to tissue engineering applications as a direct comparison has not been done and the effect that the different soluble factors (i.e. RA alone or RA and purmorphamine) and induction time periods (i.e. 6 days or 8 days) have on the generation of neurons is not evident from the current literature. There is therefore a need to determine which of the two protocols is able to generate a greater proportion of viable neurons.

For personalized neural tissue, the value of differentiation protocols is their ability to produce viable and functional iPSC-derived neurons and glia for cell-based therapy. To this end, several studies have reported positive functional outcomes from the implantation of iPSC-derived cells. Using a neural induction protocol initiated by EB formation in the presence of RA, Miura *et al.* [10] showed that iPSCs can differentiate into the three cell types of the central nervous system – neurons, oligodendrocytes, and astrocytes – without teratoma formation after implantation. In a follow-up study, appropriately evaluated "safe" iPSC-derived neural progenitor cells were implanted into a mouse spinal cord injury model where they differentiated into neural lineage cells and promoted functional recovery [11]. In another study initiating neural differentiation using EB formation, iPSC-derived dopaminergic neurons were implanted into a rat Parkinson's Disease model, contributing to improved behavioural outcomes [35]. These studies indicate the relevance of iPSC-derived cell therapies for the treatments of the damaged central nervous system.

Engineering personalized neural tissue requires the development of three-dimensional (3D) biomaterial scaffolds that can support the differentiation, growth, and survival of neurons derived from iPSCs. A key biomaterial consideration is the physical microenvironment in which cells reside and the properties of this environment have a considerable influence on cell behaviour. In many cases, materials for tissue engineering seek to emulate the extracellular matrix (ECM) of native tissue – the complex 3D environment of polysaccharides and embedded fibrous proteins that provide adhesion sites as well as important chemical and mechanical signals to the cells. Natural biomaterials, such as proteins and polysaccharides, have the advantage over synthetic polymers as they more closely mimic the ECM. The specific biomaterial scaffold holds great importance as the physical cues presented by the material can significantly alter the behaviour of pluripotent stem cells undergoing differentiation in response to soluble factors. For example, Kothapalli and Kamm [24] report that the same concentration of RA and Shh have a different effect on the differentiation of murine ESCs into neurons depending on the biomaterial scaffold used to support the cells. Enhanced motor neuron formation was demonstrated in 3D collagen scaffolds while enhanced dopaminergic neuron formation was demonstrated in 3D matrigel (heterogeneous mixture of extracellular matrix proteins) scaffolds. Such work exemplifies the synergistic interaction between soluble chemical factor exposure and matrix microenvironment.

In an effort to develop an effective cell-delivery platform for neurons derived from pluripotent stem cells, fibrin scaffolds have been extensively characterized for supporting the differentiation of mECSs into neural and glial phenotypes [36-40]. Fibrin is a protein-based biomaterial that can cause clotting of blood. Found in blood, it is produced in response to injury from the inactive zymogen fibrinogen via the immune response coagulation cascade. The final step of the cascade involves the cleavage of the fibrinogen monomer at four key locations, revealing binding sites that allow for the assembly of monomers into fibres and subsequent organization into a fibrous hydrogel network by the cross-linking action of Factor XIIIa [41]. This polymerization mechanism can be recapitulated *in vitro* or *in situ* in the presence of calcium ions and another activated blood plasma protein, thrombin. Partly owing to this functionality, fibrin was one of the first natural polymer biomaterials to be used in clinical applications, typically as a surgical sealant. It has been approved by the Food and Drug Administration (FDA) and is well characterized in terms of its biocompatibility for many different biomedical applications, including treatments for peripheral and central nerve injuries [41] [42]. These commercially available products have formed an established base upon which modifications and novel techniques can be more easily developed and translated to clinical practice.

Fibrin hydrogels can also be functionalized with other molecules or therapeutic drugs that are either associated with the fibrin protein covalently via crosslinking during polymerization or loaded within the aqueous phase. For example, in one fibrin-based drug delivery approach, peptide sequences are designed with a fibrin-binding domain consisting of a transglutaminase substrate (amino acid sequence NQEQVSPKA) at the N terminus, allowing it to be covalently incorporated in a fibrin clot via the activity of cross-linking Factor XIIIa [43]. The remaining portion of the peptide sequence can then be rationally designed to have a known binding affinity with a target therapeutic drug such that it can controls the release of the drug over time [44]. This approach is advantageous because, unlike synthetic polymer matrices where altering release kinetics often impacts mechanical and structural properties, the drug delivery can be tailored in a manner more independent of physical properties through variations in binding affinities or number of binding sites [45]. The material properties of polymerized fibrin hydrogels – such as pore size, fibre diameter, and gel stiffness – can be tailored by varying the concentrations of fibrinogen, thrombin, and calcium, and this has an effect on the fate of the cells with which the fibrin is combined [46]. The concentration of these components must therefore be optimized for each specific cell-based application. For 3D fibrin matrices that support the generation of neurons derived from pluripotent stem cells, Willerth *et al.* have previously undertaken a study to optimize the material properties, suggesting a fibrin concentration of 10 mg/mL [36].

Given these established advantages, the generation of neurons inside fibrin scaffolds continues to be a promising strategy for spinal cord injury repair. However, previous work has focussed exclusively on murine ESCs while the translation of the fibrin-based platform for use with iPSCs remains unexplored. Adapting these existing

protocols to new cell types and demonstrating the successful application of 3D fibrin scaffolds for the differentiation of iPSCs into neurons is an important step forward. This study therefore aims to successfully culture murine iPSCs inside 3D fibrin scaffolds, while determining which of the two EB formation protocols is more suitable for this application in terms of the level of cell viability and proportion of neurons generated.

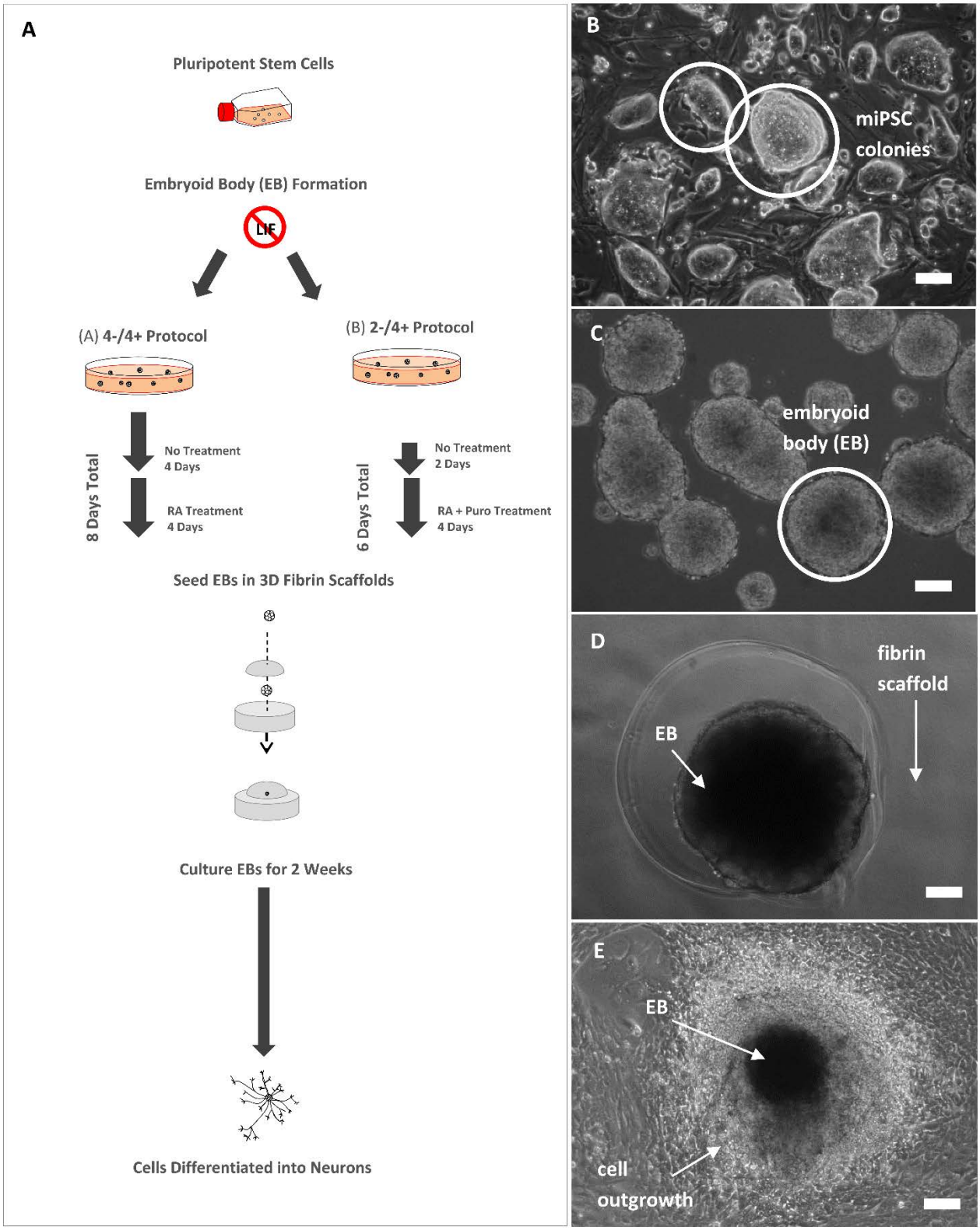

Figure 1 Schematic representation of embryoid body (EB) formation and seeding inside 3D fibrin scaffolds. (A) Schematic outline of EB formation and seeding in 3D fibrin scaffolds. Pluripotent murine stem cell colonies (B) are removed from routine culture and induced to form embryoid bodies (EBs) (C) using either the 8-day 4-/4+ protocol with retinoic acid (RA) treatment in the last 4 days or the 6-day 2-/4+ protocol with RA and purmorphamine (Puro) treatment in the last 4 days. EBs are then seeded inside 3D fibrin scaffolds (D) and cultured for 2 weeks to support differentiation into neurons (E). Scale bars are 100 μm.

2 Results and discussion

2.1 Viability assessment

In this study, cell viability is defined as the proportion of viable cells out of the total measured cell population. Viable cells are considered to be those cells exhibiting fluorescence as measured by the Millipore Guava ViaCount assay (uses a combination of proprietary DNA-binding dyes to indicate live, apoptotic, and dead cells) and by using a standard Live/Dead assay for qualitative images. Viability is reported as mean ± standard deviation. Because the total number of cells in each sample can vary, relative rather than absolute metrics of viability are reported to normalize for variation in EB size. Although it was not considered in our study, the overall yield of viable cells may be manipulated through control of EB size prior to seeding (using an EB formation technology such as AggreWell® microwell plates) or increasing the quantity of EBs seeded.

Cell viability is high at completion of EB formation and prior to seeding. Both miPSC- and mESC-derived EBs exhibited high level of viability at the point of formation. Furthermore, regardless of cell type, both the 4-/4+ and 2-/4+ differentiation protocols generated EBs with a high proportion of viable cells. For miPSC-derived EBs, those formed using the 4/4+ protocol yielded 92%±1% viable cells while those formed using the 2-/4+ protocol yielded 89%±2% viable cells, based on flow cytometry-based viability analysis prior to seeding. For mESC-derived EBs, those formed using the 4/4+ protocol yielded 89%±5% viable cells while those formed using the 2-/4+ protocol yielded 87%±3% viable cells prior to seeding. No significant difference was observed between the four different experimental conditions. As shown in Figure 2 below, no qualitative differences in the level of viability were apparent between different cell lines or differentiation protocols based on LIVE/DEAD® staining.

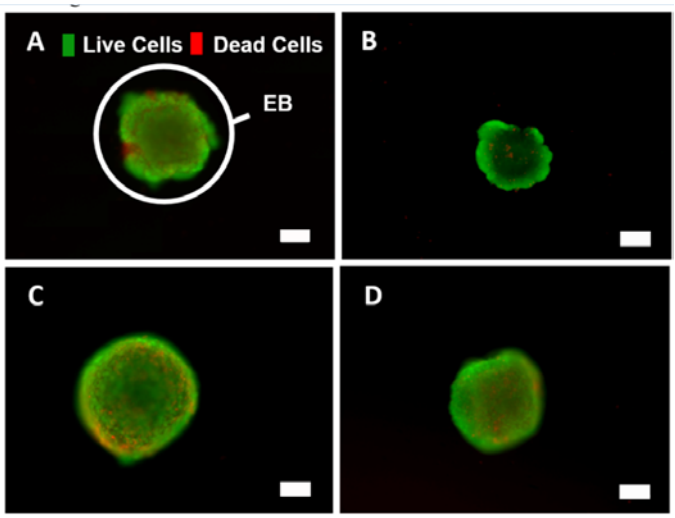

Figure 1 Fluorescent LIVE/DEAD® images showing high levels of viability for iPSC- and ESC-derived 4-/4+ and 2-/4+ EBs at completion of EB formation Fluorescent images of (A) iPSC-derived 4-/4+ EB, (B) iPSC-derived 2-/4+ EB, (C) ESC-derived 4-/4+ EB, and (D) ESC-derived 2-/4+ EB, at completion of the EB formation protocols and prior to seeding inside of fibrin scaffolds. Green indicates live cells and red indicates dead cells. Scale bars are 100 μm.

2.1.1 **Cells viability remains high after 14 days of culture inside 3D fibrin scaffolds.** EBs generated from both cell lines and both differentiation protocols survive and give rise to viable cells after culture inside 3D fibrin scaffolds for 14 days. For miPSC-derived EBs, the 4/4+ protocol yielded 89%±7% viable cells while those formed using the 2-/4+ protocol yielded 90%±10% viable cells, based on flow cytometry-based viability analysis at day 14. For mESC-derived EBs, the 4/4+ protocol yielded 91%±10% viable cells while those formed using the 2-/4+ protocol yielded 89%±10% viable cells at day 14. No significant differences were observed in viability between the four different experimental conditions. As shown in Figure 3, substantial cell outgrowth from the EB into the fibrin matrix is achieved by day 14 and no qualitative differences in viability were apparent between the cell lines of differentiation protocols based on LIVE/DEAD® staining.

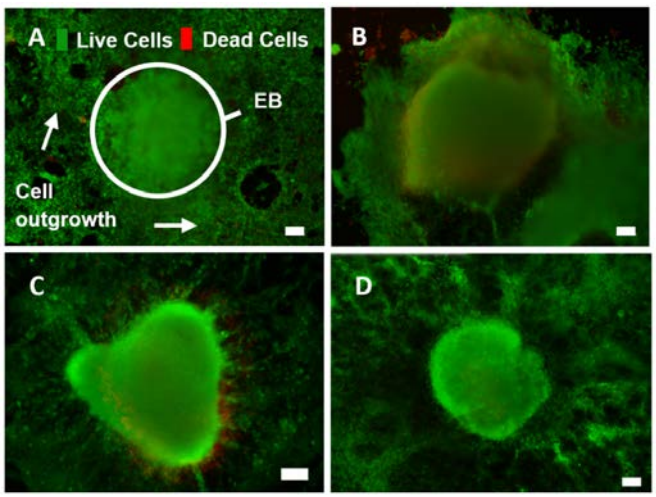

Figure 2 Fluorescent LIVE/DEAD® images showing high viability for all EBs after 14 days of culture in fibrin scaffolds Fluorescent LIVE/DEAD® images for **(A)** iPSC-derived 4-/4+ EB, **(B)** iPSC-derived 2-/4+ EB, **(C)** ESC-derived 4-/4+ EB, **(D)** ESC-derived 2-/4+ EB after 14 days of culture inside of 3D fibrin scaffolds. Green indicates live cells and red indicates dead cells. Scale bars are 100 μm.

The viability data is shown graphically in Figure 3 with no significance differences in the level of viability were measured. Furthermore, no significant change in viability was measured over the 14 day culture period. The sustained high levels of viability measured in the miPSC populations over the culture period indicate that these cells can indeed be successfully combined with the fibrin-based cell-delivery platform for neural tissue engineering applications.

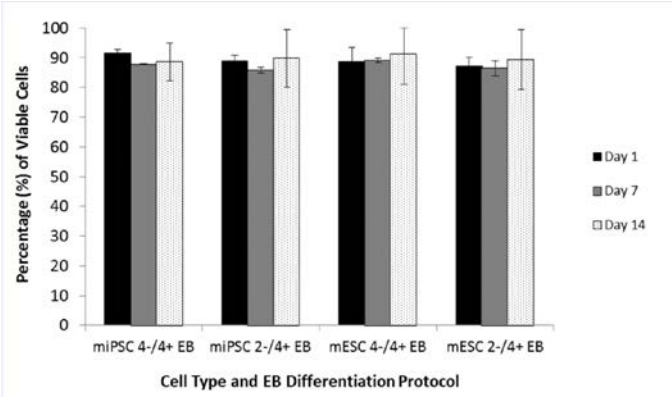

Figure 3 Quantitative viability results for cells cultured inside of 3D fibrin scaffolds. Percentage of viable cells measured by flow cytometry for miPSC 4-/4+ and 2-/4+ EBs and mESC 4-/4+ and 2-/4+ EBs at day 1, day 7, and day 14 of culture inside 3D fibrin scaffolds. No significant differences were measured between cell types or differentiation protocols over the 14 day culture period. Error bars show SEM. Sample size n = 2.

2.2 Efficiency of Neuronal Differentiation

Neuronal differentiation efficiency is defined as the proportion of neuronal cells generated from the seeded EBs out of the total cell population. Neuronal cells are considered to be those cells expressing early neuronal marker β-III-tubulin (TUJ1) as measured by flow cytometry and immunocytochemistry techniques. Because the number of cells in each EBs is not known at the time of seeding, relative (rather than absolute) metrics of neuronal differentiation are reported to normalize for variation in EB size as detailed for the viability.

2.2.1 **Expression of early neuronal marker TUJ1 after 14 days of culture in 3D fibrin scaffolds.** This study focuses on the generation of neurons as these cells are desirable for the treatment of many neurological disease and disorders. The results provide the first reported assessment of the neuronal differentiation of miPSCs using this biomaterial platform. After 14 days of culture inside 3D fibrin scaffolds, the percentage of TUJ1-positive immature neuron cells generated from the 2-/4+ protocol was determined to be significantly higher than those generated from the 4-/4+ protocol for both iPSC- and ESC-derived EBs, as shown in Figure 4A. At the end of the culture period, the TUJ1 expression for miPSC 2-/4+ cells was 23%±4% while expression for miPSC 4-/4+ cells was only 17%±1%. The TUJ1 expression for mESC 2-/4+ cells was 36%±5% while expression for mESC 4-/4+ cells was only 20%±1%. Note that the proportion of mESC-derived TUJ1-positive early neuronal cells generated from the 4-/4+ EB formation protocol in this study were consistent with previously reported values, including studies by Willerth *et al.* [37, 38] which show between 10% to 20% TUJ1-positive cells from mESC-derived 4-/4+ EBs after 2 weeks of culture in fibrin scaffolds with no neurotrophic factor exposure.

Both iPSC- and ESC-derived EBs generated from 2-/4+ and 4-/4+ differentiation protocols show a significant increase in TUJ1 expression between day 7 and day 14, as shown quantitatively in Figure 4A. For miPSCs, EBs generated from the 2-/4+ protocol had 11%±6% cells expressing TUJ1 at day 7, increasing to 23% ±4% by day 14, while those generated from the 4-/4+ protocol had only 8%±2% of cells expressing TUJ1 at day 7, increasing to only 17%±1% at day 14. For mESC-derived EBs, those generated from the 2-4+ protocol had 13%±6% cells expressing TUJ1 at day 7, increasing to 36%±5% by day 14, while the EBs generated from the 4-/4+ protocol had only 10%±3% cells expressing TUJ1 by day 7, increasing to only 20%±1% by day 14. These results are also confirmed qualitatively by the TUJ1-positive stained cells shown in Figure 5.

As with many differentiation protocols for murine stem cells, the 14-day time period for neuronal differentiation in fibrin was previously developed using mESCs, specifically 4-/4+ mESC-derived EBs [36-38]. The 14-day time period was determined by the length of time that fibrin is typically able to persist in culture before substantial degradation by cell-secreted proteases. Given the comparable degree of neuronal differentiation measured across all experimental conditions, the results of this study suggest that adjustment of the 14-day culture period is not required to capture the behaviour of miPSCs or EBs generated by the 2-/4+ protocol, which is a useful outcome to consider for the development of future studies investigating miPSCs in fibrin scaffolds.

2.2.2 **Expression of neural progenitor marker nestin after 14 days in 3D fibrin scaffolds.** Nestin is an intermediate filament protein commonly used as a marker for neural progenitor cells. As pluripotent cells begin to differentiate into neurons, they first pass through the neural progenitor phase, indicated by high levels of nestin expression, before further specializing into neurons, indicated by a diminished level of nestin expression and an increase in TUJ1 expression. Accordingly, nestin may be considered as an indicator of future neuronal differentiation. However, it is important to note that while all neurons are derived from nestin-expressing neural progenitor cells, not all nestin-expressing cells necessarily become neurons. It is therefore important to consider nestin expression levels in the context of other markers, such as TUJ1.

The percentage of nestin-positive cells generated from the 2-/4+ protocol was determined to be significantly higher compared to those generated from the 4-/4+ protocol for both cell types. At day 14, nestin expression for miPSC-derived 2-/4+ EBs was 13%±6% while expression for miPSC-derived 4-/4+ EBs was only 9%±2%SD. Similarly, for mESC-derived 2-/4+ EBs, the percentage of nestin-positive cells was 17%±5% while only 10%±4% for the mESC-derived 4-/4+ EBs. These results, summarized in Figure 4B, are an indication of the population of neural progenitor cells at day 7 and day 14 of the culture period. As expected, the nestin expression decreases from day 7 to day 14 as the cells undergo differentiation from progenitor cells into neurons.

The 2-/4+ protocol yields higher levels of both nestin expression and TUJ1 expression than the 4-/4+ protocol. Given that both the nestin and TUJ1 expression levels are higher, it suggests a greater degree of overall differentiation for the 2-/4+ protocol (whereas, higher levels of nestin expression alone would instead be an indication of less effective differentiation following the progenitor phase). In this

context, the higher levels of nestin expression at day 7 indicates the future capacity of the cell populations to further differentiate into neurons by day 14. In addition, the remaining progenitor cells at the end of the 14-day culture period have the ability to further differentiate and contribute to the neuronal cell population. Thus, in tandem with the higher levels of TUJ11, the higher levels of nestin expression measured for the 2-/4+ EBs provides further evidence for the effectiveness of this protocol for generating neurons inside 3D fibrin matrices.

2.2.3 **Comparing the expression of neural markers between EBs derived from iPSCs and ESCs for both differentiation protocols.** After 14 days, the percentage of TUJ1-positive cells is higher in ESC-derived EBs compared to iPSC-derived EBs for both protocols, which is consistent with previous studies reporting lower differentiation efficiency for iPSCs [12]. These previous studies propose that epigenetic factors, such as levels of histone modification, may be playing a role in the reduced ability of iPSCs to differentiate compared to ESCs. Indeed, histone modifications are an extremely important consideration for iPSCs and have been shown to block iPSC reprogramming, as demonstrated by Rais *et al.* [8] in their study achieving nearly 100% reprogramming efficiency.

Our study suggests that purmorphamine has the ability to increase the proportion of neurons generated from the 2-/4+ EBs compared to the 4-/4+ EBs, there remains a decreased level of neuronal differentiation by miPSCs relative to mECSs. Given what is currently known about the differences between miPSCs and mESCs, it is likely due to the overall reduced differentiation efficiency of miPSCs due to epigenetic factors.

For both 2-/4+ and 4-/4+ iPSC-derived EBs, the increase in TUJ1 expression from day 7 to day 14 is accompanied by a significant decrease in the expression of neural progenitor marker nestin as well as pluripotency marker SOX2 (Figures 4A, 4B, and 4C respectively). SOX2 is a common marker for pluripotency in stem cells. However, given that it is one of the induced factors used in the generation of the miPSC line, it is not generally considered to be the most robust indicator of pluripotency. The measured levels of SOX2 may include residual expression and not necessarily reflect the changes in expression that may be occurring due to differentiation. However, SOX2 expression can still provide useful insight when considered in the context of other markers such as TUJ1 and nestin. The observed pattern of nestin and SOX2 expression is consistent with the expectation that the transient expression of nestin decreases [47] and that the overall proportion of undifferentiated cells expressing SOX2 decreases [48] as the cells specialize down neuronal lineages. Interestingly, for the ESC-derived EBs, the observed decreases in nestin and SOX2 expression over this time period were not significant. Additional differences in the behaviour of miPSC- and mESC-derived EBs can be seen in how the cells respond to the two differentiation protocols. For example, the mESC-derived EBs show a significant difference in nestin and SOX2 expression between the 2-/4+ and 4-4+ protocols at day 7 and day 14 but these differences do not emerge in the miPSC-derived EBs until day 14. Thus, the effects of the 2-/4+ protocol appear to take longer to emerge in the miPSC-derived EBs.

Lastly, for the 2-/4+ protocol, the SOX2 expression is significantly different between miPSC- and mESC-derived EBs at day 7 but the difference is diminished by day 14. The same effect is observed for the EBs generated using the 4-/4+ protocol, suggesting that the effects on differentiation take longer in the miPSC-derived EBs. While iPSCs and ESCs use the same signalling pathways when differentiating into neural phenotypes, high variability in differentiation efficiency is observed between different cell lines, regardless of whether they are iPSCs or ESCs [7, 12, 49]. Thus, it may be possible to attribute the differences between the miPSC- and mESC-derived EBs to differences between the specific cell lines rather than as representing general differences between iPSCs and ESCs.

2.2.4 **Implications for fibrin-based neural tissue engineering** It should also be noted that the TUJ1-, nestin-, and SOX2-positive cells reported in Figure 5 and Figure 6 do not represent mutually exclusive populations and, furthermore, these cells do not account 100% of the total cell population. Making up the balance of cells unaccounted for must therefore be cells differentiating into non-neuronal cell types. The presence of undifferentiated and undesirable phenotypes remains problematic for stem-cell based clinical applications where a high quality population of one or even multiple desired cell types are needed. For example, Johnson *et al.*[40] transplanted mESC-derived EBs along with fibrin scaffolds containing neurotrophic factors in a rat spinal cord injury model where these factors promoted cellular proliferation. When the fibrin scaffolds were functionalized with an affinity-based drug delivery system for the neurotrophic factors, even more proliferation was achieved. Unfortunately, the increased proliferation occurred in the non-neural/non-glial population (estimated to be approximately 30% of the implanted cells) and ultimately led to reduced functional recovery in the affected animals. This study underscores the importance of achieving a pure population of the desired cell types for stem-cell based therapies and highlights the importance of removing undifferentiated pluripotent stem cells before transplantation.

In our study, the detected SOX2 expression at the end of the 14-day culture period indicates that a degree of heterogeneity in the population persists even in the presence of the improved 2-/4+ retinoic acid and purmorphamine based differentiation approach, suggesting undifferentiated cells are still present. Further optimization of neuronal differentiation protocols for murine iPSCs in fibrin. Cell sorting to remove the undifferentiated cells prior to combination with the fibrin cell-delivery platform may also be required, although this approach has its own challenges. Notably, the introduction of fluorescent markers or bacterial resistance genes for sorting techniques may cause inadvertent genomic manipulation through selection and thus increase the associated tumorigenic risks.[50]. This process can also be harsh on the cells and may decrease viability of the sorted cells once seeded inside of the scaffold.

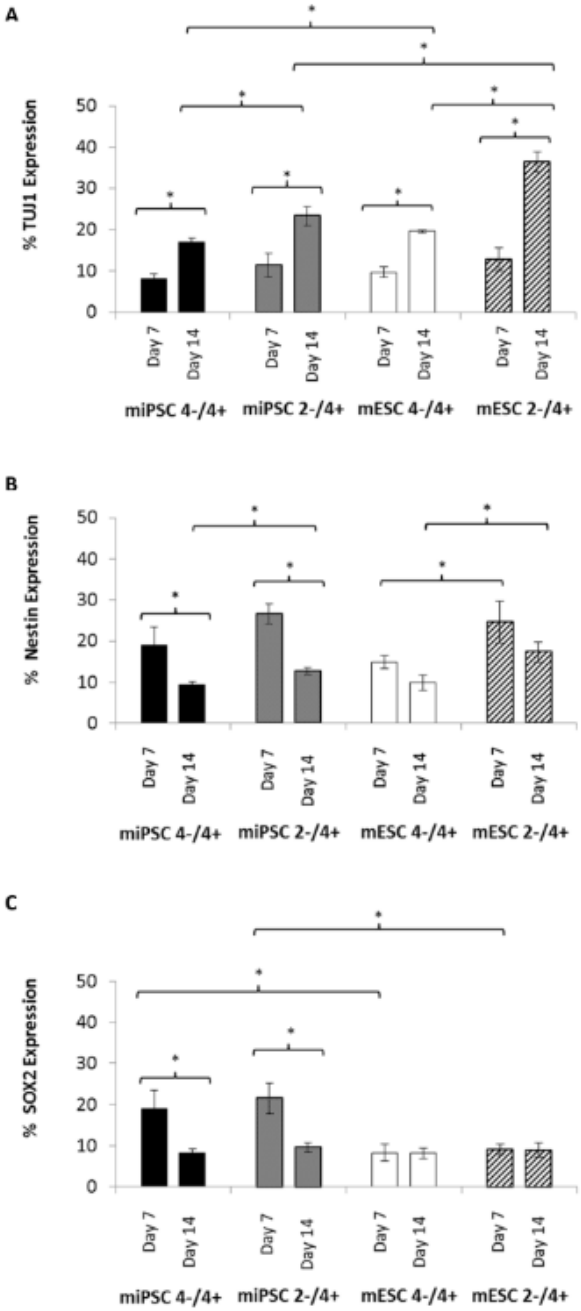

Figure 4 Expression of early neuronal marker TUJ1, neural progenitor marker nestin, and pluripotency marker SOX2 after 7 days and 14 days of culture in fibrin Relative marker expression in percent (%) at day 7 and day 14 for the four experimental conditions: miPSC-derived 4-/4+ EBs, miPSC-derived 2-/4+ EBs, mESC-derived 4-/4+ EBs, and mESC-derived 2-/4+ EBs. (A) Early neuronal marker β-III-tubulin (TUJ1). (B) Neural progenitor marker nestin. (C) Pluripotency marker SOX2. Error bars show SEM. Sample size n = 4. * indicates $p < 0.05$.

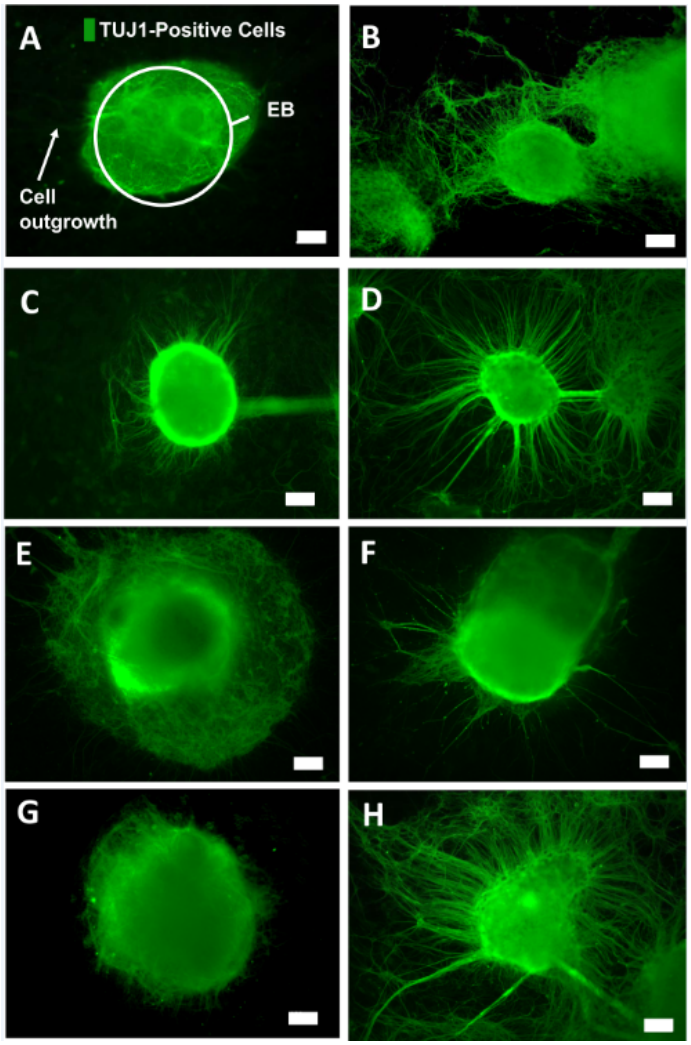

Figure 5 Early neuronal marker TUJ1-positive cells after 7 days (A,C,E,G) and 14 days (B,D,F,H) of culture in fibrin Cell outgrowth stained positive for early neuronal marker β-III-tubulin (TUJ1) for iPSC-derived 4-/4+ EBs at (A) day 7 and (B) day 14; iPSC-derived 2-/4+ EBs at (C) day 7 and (D) day 14; ECS-derived 4-/4+ EBs at (E) day 7 and (F) day 14; and ESC-derived 2-/4+ EBs at (G) day 7 and (H) day 14. Scale bars are 100 μm.

3 Conclusion and future work

We have demonstrated the successful translation of the fibrin-based cell-delivery platform for use with neural progenitors derived from murine iPSCs. Given that miPSCs have been reported to differentiate into desired cell phenotypes less effectively than ESCs, our work included a comparison of two neuronal differentiation protocols with the aim of developing a protocol to maximize the production of neurons inside of 3D fibrin scaffolds. Accordingly, we demonstrated that EBs generated using the 6-day 2-/4+ protocol generate a higher proportion of neuronal cells compared to the more traditional 8-day 4-/4+ protocol when seeded inside 3D fibrin scaffolds for 14 days. A proportional metric was used to normalize for the heterogeneous sizes of the EBs that were initially seeded.

Consistent with previous reports, the overall differentiation efficiency (i.e. the proportion of differentiated cells compared to the total cell population) was determined to be lower in iPSCs compared to ESCs. However, we show that the application of the 2-/4+ protocol can counteract some of this effect for iPSC-derived EBs seeded in fibrin by increasing the proportion of neurons generated compared to the traditional RA only protocol. These results provide evidence to support the use of the 2-/4+ protocol as a faster, more efficient method of EB formation for downstream differentiation of murine iPSCs into neurons in conjunction with fibrin-based scaffold for cell-delivery applications.

Future work will also further refine the protocol with a more detailed analysis of the synergistic effects of RA and purmorphamine in the 3D biomaterial scaffold environment along with translating these protocols for use with neural progenitors cells derived from human iPSCs. The results of this additional characterization would also support protocols for the differentiation of human pluripotent cell lines in 3D fibrin cell-delivery platforms, as existing 2D methods involve varying combinations of soluble RA and Shh agonists [26, 29, 51]. One of the main advantages of fibrin as a biomaterial for cell delivery is the versatility of the matrix to incorporate affinity-based drug delivery systems. In the future, we will also adapt neurotrophic factor drug delivery systems to further support the differentiation and survival of 2-/4+ iPSC-derived neurons inside of fibrin scaffolds.

4 Materials and methods

4.1 Materials

The stem cell media used contains Dulbecco's Modified Eagle Medium (DMEM) High Glucose No Glutamine (Life Technologies), 15% ES-cell qualified fetal bovine serum (FBS) (Life Technologies), 0.1 mM MEM Non-Essential Amino Acids (Life Technologies), 2 mM GlutaMAX™ Supplement (Life Technologies), 0.055mM β-mercaptoethanol, 0.1 mM nucleosides (Millipore),100 µg/mL Penicillin-Streptomycin (Life Technologies). Other cell culture materials include EmbryoMax 0.1% gelatin solution, Leukemia Inhibitory Factor (LIF) (Millipore), 0.25% Trypsin-EDTA (Life Technologies), agar (Sigma), retinoic acid (RA) (Sigma) reconstituted in ethanol, purmorphamine (StemGent) reconstituted in dimethylsulfoxide (DMSO) (Sigma), lyophilized human fibrinogen (Calbiochem) reconstituted in tris-buffered saline (TBS), lyophilized bovine thrombin (Sigma) reconstituted in TBS, anhydrous calcium chloride (Sigma) reconstituted in TBS, NeuralBasal Media (Life Technologies), and B27 Supplement (Life Technologies). Mitotically inactivated mouse embryonic fibroblasts (MEF) (CF-1) were supplied GlobalStem. Murine iPSCs were supplied by Systems Bioscience. Murine ESCs (R1 line) were supplied by the Nagy Lab at the University of Toronto. Flow cytometry materials include the FlowCellect Rodent NSC Characterization Kit (Millipore). Cell viability assay materials include LIVE/DEAD® Cell Viability/Cytotoxicity Kit (Life Technologies) and Guava Viacount Reagent (Millipore). Immunocytochemistry materials include primary anti-β-III-tubulin (TUJ1) (Millipore), secondary Alexa Fluor488 goat anti-mouse IgG (Life Technologies), 10% formalin (Sigma), Triton-X (Sigma), and normal goat serum (NGS) (Millipore).

4.2 Cell culture protocols

4.2.1 **Maintenance of pluripotent cells.** Murine iPSCs and ESCs were cultured on a feeder layer of MEF and 0.1% gelatin in the presence of stem cell media with 1000 U/mL LIF. Cells were passaged enzymatically with trypsin approximately every 2 days at a ratio of 1:5. Cells were maintained at 37˚C and 5% CO_2 throughout routine culture and differentiation protocols.

4.2.2 **Differentiation protocols.** To initiate embryoid body formation, approximately 5 x 10^4 cells/mL suspended in stem cell media without LIF were plated onto non-adherent 0.1% agar-coated polystyrene cell culture dishes. For the 8-day 4-/4+ protocol, embryoid bodies are formed for 4 days without treatment followed by 4 days in the presence of 500 nM RA. For the 6-day 2-/4+ protocol, embryoid bodies are formed for 2 days without treatment followed by 4 days in the presence of 500 nM retinoic acid and 1 mM purmorphamine. Media was changed every 2 days for both protocols.

4.2.3 **Seeding EBS inside 3D fibrin scaffolds.** EBs were seeded inside 3D fibrin scaffolds as previously described [52]. Briefly, 10 mg/mL sterile fibrinogen was polymerized in the presence of 40 U/mL thrombin and 50 mM $CaCl_2$ in the wells of a 24-well polystyrene cell culture plate; single EBs were seeded on the surface of a 300 µL fibrin gel with another 100 µL fibrin gel subsequently polymerized on top. Following seeding, 1 mL of stem cell media was added to each well. Media was changed to NeuralBasal Media with B27 Supplement after 3 days. The change in media is undertaken after the cells have adapted to the new culture environment in order to present a serum-free environment that will support differentiation and maintain neurons. EBs were maintained for 2 weeks before harvesting for flow cytometry or fixation for immunocytochemistry.

4.3 Flow cytometry

4.3.1 **Preparation of cell suspension.** Cells were isolated from inside the 3D fibrin scaffolds and dissociated enzymatically using exposure to trypsin for 20 minutes at room temperature. Trypsinized cells were quenched with stem cell media, washed with PBS, and passed through a 60 µm strainer to ensure a single cell suspension.

4.3.2 **Viacount assay.** Cell viability and concentration were measured using the Guava ViaCount assay. Cell suspensions were diluted 1:10 in the Guava ViaCount Reagent and incubated for 5 minutes at room temperature protected from light. Data was collected using a Guava® EasyCyte HT (Millipore) flow cytometer.

Gating was performed within the ViaCount application to separate live and dead cells. Cell suspensions were diluted to approximately 500 cells/mL for further analysis.

4.3.3 **Staining.** Cells stained for early neuronal marker TUJ1, neural progenitor marker Nestin, and pluripotency marker SOX2 were then prepared according to the directions of the FlowCellect Rodent NSC Characterization Kit. Briefly, cells were incubated in the Fixation Buffer for 20 minutes at room temperature, washed and incubated in Permeabilization Buffer with fluorescent stains for 1 hour on ice; each sample was subdivided and treated with a single target marker or isotype control. Stains included directly conjugated TUJ1-PE-CY5, IgG2a-PE-CY3 isotype control, Nestin-PE, IgG1-PE isotype control, SOX2-FITC, and IgG2A-FITC isotype control. Samples were washed and resuspended in Assay Buffer for analysis.

4.3.4 **Flow cytometry analysis.** Data was collected using a Guava® EasyCyte HT (Millipore) flow cytometer. Gating was performed to exclude debris and doublet cells. Gain controls were set for each isotype control such that fluorescence intensity above 10^1 was minimized. Each sample was collected up to a maximum of 5000 gated events. Data analysis was performed using GuavaSoft InCyte software.

4.4 Cell viability

4.4.1 **LIVE/DEAD® sample preparation.** Samples were stained for viability using the LIVE/DEAD® Viability/Cytotoxicity Kit. Briefly, samples were incubated in PBS containing 2 μM calcein-AM and 4 μM ethidium homodimer (EthD-1). In live cells, the calcein-AM passes through the cell membrane where it is cleaved into fluorescent calcein by intracellular esterase activity. EthD-1 is excluded from live cells due to its size; however, it penetrates the ruptured membranes of dead cells and binds to nucleic acids which then causes an amplification of its fluorescence.

4.4.2 **Imaging.** Fluorescent images were obtained on a Leica DMI 3000B microscope with a QImaging RETIGA 2000R camera at a magnification of 100X. GFP and CY3 filters were used for fluorescent excitation (green and red channels). QCapture software was used for image capture. Phase contrast and fluorescent images were captured for each sample. Green and red channel images were merged using Adobe PhotoShop Extended CS5 software with the opacity of the layers at 50%.

4.5 Immunocytochemistry

4.5.1 **Sample preparation.** Cells inside 3D fibrin were washed with PBS and fixed with 10% formalin for 1 hour at room temperature and then permeabilized with 0.1% Triton-X for 45 minutes at 2 – 8 ˚C. Wells were blocked with 5% NGS for 2 hours at 2 – 8 ˚C. Primary antibody TUJ1-IgG was added at a dilution of 1:500 and incubated at 2 – 8 ˚C overnight. Cells were washed 3 times with PBS including a 15 minute incubation at 2 – 8 ˚C between each wash. The secondary antibody was added at a dilution of 1:200 and incubated for 4 hours at room temperature. Cells were again washed 3 times with PBS including a 15 minute incubation at 2 – 8 ˚C between each wash. Additional PBS was added to each well to prevent drying of the samples for imaging.

4.5.2 **Imaging.** Fluorescent images were obtained on a Leica DMI 3000B microscope with a QImaging RETIGA 2000R camera at a magnification of 100X; a GFP filter was used for fluorescent excitation (green channel). QCapture Suite (QImaging) software was used for image capture. Both phase contrast and fluorescent images were captured for each sample.

4.6 Statistical analysis

4.6.1 **Sample size** Sample sets represented the four experimental conditions (miPSC 4-/4+, miPSC 2-/4+, mESC 4-/4+, and mESC 2-/4+) at two separate time points (7 days and 14 days). Overall, this included data from eight separate 24-well plates, four of which were harvested after day 7 and four of which were harvested after day 14. Each 24-well plate contained 6 wells prepared for each experimental condition. Cells from the 6 wells were pooled into one sample in order to obtain sufficient cells for analysis.

4.6.2 **Test for normality.** In order to determine whether or not the results were normally distributed and therefore eligible for analysis by methods that assume this distribution, sample sets were first tested for normality using the one sample Kolmogorov-Smirnov (K-S) test. Results were determined to a 5% significance level.

4.6.3 **Tests for significance.** As none of the results data was determined to exhibit a normal distribution, significant differences between sample sets were tested using methods which do not assume an underlying normal distribution – namely, the two sample K-S test and the Kruskal-Wallis (K-W) one-way analysis of variance test. Results were determined to a 5% significance level for both tests. Standard deviation (SD) and standard error of the mean (SEM) are reported as percent (%).

Acknowledgements

The authors would like to acknowledge the National Sciences and Engineering Council (NSERC) funding from their Discovery, Engage and Research Tools and Instrument grant programs for supporting this work.

References

1. Evans, M.J. and M.H. Kaufman, *Establishment in culture of pluripotential cells from mouse embryos.* Nature, 1981. **292**(5819): p. 154-156.
2. Martin, G.R., *Isolation of a pluripotent cell line from early mouse embryos cultured in medium conditioned by teratocarcinoma stem cells.* Proceedings of the National Academy of Sciences, 1981. **78**(12): p. 7634-7638.
3. Thomson, J.A., et al., *Embryonic stem cell lines derived from human blastocysts.* Science, 1998. **282**: p. 1145-1147.

4. Takahashi, K. and S. Yamanaka, *Induction of pluripotent stem cells from mouse embryonic and adult fibroblast cultures by defined factors.* Cell, 2006. **126**(4): p. 663-76.
5. Takahashi, K., et al., *Induction of pluripotent stem cells from adult human fibroblasts by defined factors.* Cell, 2007. **131**(5): p. 861-72.
6. Yu, J., et al., *Induced pluripotent stem cell lines derived from human somatic cells.* Science, 2007. **Scienceexpress Report**: p. 1-4.
7. Yamanaka, S., *Induced pluripotent stem cells: past, present, and future.* Cell Stem Cell, 2012. **10**: p. 678-684.
8. Rais, Y., et al., *Deterministic direct reprogramming of somatic cells to pluripotency.* Nature, 2013. **502**(7469): p. 65-70.
9. Okita, K., et al., *Generation of Mouse Induced Pluripotent Stem Cells Without Viral Vectors.* Science, 2008. **322**(5903): p. 949-953.
10. Miura, K., et al., *Variation in the safety of induced pluripotent stem cell lines.* Nat Biotech, 2009. **27**(8): p. 743-745.
11. Tsuji, O., et al., *Therapeutic potential of appropriately evaluated safe-induced pluripotent stem cells for spinal cord injury.* Proc Natl Acad Sci U S A, 2010. **107**(28): p. 12704-9.
12. Hu, B.-Y., et al., *Neural differentiation of human induced pluripotent stem cells follows developmental principles but with variable potency.* Proceedings of the National Academy of Sciences, 2010. **107**(9): p. 4335-4340.
13. Tokumoto, Y., et al., *Comparison of efficiency of terminal differentiation of oligodendrocytes from induced pluripotent stem cells versus embryonic stem cells in vitro.* J Biosci Bioeng, 2010. **109**(6): p. 622-8.
14. Löhle, M., et al., *Differentiation Efficiency of Induced Pluripotent Stem Cells Depends on the Number of Reprogramming Factors.* Stem Cells, 2012. **30**(3): p. 570-579.
15. Willerth, S.M., *Neural tissue engineering using embryonic and induced pluripotent stem cells.* Stem Cell Res Ther, 2011. **2**(2): p. 17.
16. Martin, G.R. and M.J. Evans, *Differentiation of clonal lines of teratocarcinoma cells: formation of embryoid bodies in vitro.* Proceedings of the National Academy of Sciences, 1975. **72**(4): p. 1441-1445.
17. Bain, G., et al., *Embryonic stem cells express neuronal properties in vitro.* Developmental Biology, 1995. **168**(2): p. 11307-11312.
18. Maden, M., *Retinoic acid in the development, regeneration and maintenance of the nervous system.* Nature Reviews Neuroscience, 2007. **8**: p. 755-765.
19. Rhinn, M. and P. Dollé, *Retinoic acid signalling during development.* Development, 2012. **139**(5): p. 843-858.
20. Ericson, J., et al., *Two critical periods of Sonic Hedgehog signaling required for the specification of motor neuron identity.* Cell, 1996. **87**(4): p. 661-73.
21. Briscoe, J. and J. Ericson, *The specification of neuronal identity by graded sonic hedgehog signalling.* Seminars in Cell & Developmental Biology, 1999. **10**(3): p. 353-362.
22. Wichterle, H., et al., *Directed differentiation of embryonic stem cells into motor neurons.* Cell 2002. **110**: p. 385-397.
23. Miles, G.B., et al., *Functional Properties of Motoneurons Derived from Mouse Embryonic Stem Cells.* The Journal of Neuroscience, 2004. **24**(36): p. 7848-7858.
24. Kothapalli, C.R. and R.D. Kamm, *3D matrix microenvironment for targeted differentiation of embryonic stem cells into neural and glial lineages.* Biomaterials, 2013. **34**(25): p. 5995-6007.
25. Brown, C.R., et al., *Generation of V2a interneurons from mouse embryonic stem cells.* Stem Cells and Development, 2014.
26. Li, X.-J., et al., *Directed differentiation of ventral spinal progenitors and motor neurons from human embryonic stem cells by small molecules.* Stem Cells, 2008. **26**: p. 886-893.
27. Stacpoole, S., et al., *Efficient derivation of NPCs, spinal motor neurons and midbrain dopaminergic neurons from hESCs at 3% oxygen.* Nature protocols, 2011. **6**(8): p. 1229-1240.
28. Hu, B.-Y. and S.-C. Zhang, *Differentiation of spinal motor neurons from pluripotent human stem cells.* Nature protocols, 2009. **4**(9): p. 1295-1304.
29. Li, X.-J., et al., *Specification of motoneurons from human embryonic stem cells.* Nature biotechnology, 2005. **23**(2): p. 215-221.
30. Sinha, S. and J.K. Chen, *Purmorphamine activates the hedgehog pathway by targeting smoothened.* Nature Chemical Biology, 2006. **2**(1): p. 29-30.
31. Briscoe, J., *Agonizing hedgehog.* Nature Chemical Biology, 2006. **2**(1): p. 10-11.
32. El-Akabawy, G., et al., *Purmorphamine increases DARPP-32 differentiation in human striatal neural stem cells through the hedgehog pathway.* Stem Cells and Development, 2011. **20**(1): p. 1873-1887.
33. Pellett, S., et al., *Sensitive and quantitative detection of botulinum neurotoxin in neurons derived from mouse embryonic stem cells.* Biochem Biophys Res Commun, 2011. **404**(1): p. 388-92.
34. McCreedy, D.A., et al., *Transgenic enrichment of mouse embryonic stem cell-derived progenitor motor neurons.* Stem Cell Research, 2012. **8**: p. 368-378.
35. Wernig, M., et al., *Neurons derived from reprogrammed fibroblasts functionally integrate into the fetal brain and improve symptoms of rats with Parkinson's disease.* Proceedings of the National Academy of Sciences, 2008. **105**(15): p. 5856-5861.
36. Willerth, S.M., et al., *Optimization of fibrin scaffolds for differentiation of murine embryonic stem cells into neural lineage cells.* Biomaterials, 2006. **27**(36): p. 5990-6003.
37. Willerth, S.M., et al., *The effects of soluble growth factors on embryonic stem cell differentiation inside of fibrin scaffolds.* Stem Cells, 2007. **25**(9): p. 2235-44.
38. Willerth, S.M., A. Rader, and S.E. Sakiyama-Elbert, *The effect of controlled growth factor delivery on embryonic stem cell differentiation inside fibrin scaffolds.* Stem Cell Res, 2008. **1**(3): p. 205-18.
39. Johnson, P.J., et al., *Controlled release of neurotrophin-3 and platelet-derived growth factor from fibrin scaffolds containing neural progenitor cells enhances survival and differentiation into neurons in a subacute model of SCI.* Cell Transplant, 2010. **19**(1): p. 89-101.
40. Johnson, P.J., et al., *Tissue-engineered fibrin scaffolds containing neural progenitors enhance functional recovery in a subacute model of SCI.* Soft Matter, 2010. **6**(20): p. 5127-5137.
41. Doolittle, R.F., *Fibrinogen and Fibrin*, in *eLS*. 2001, John Wiley & Sons, Ltd.

42. Ahmed, T.A., E.V. Dare, and M. Hincke, *Fibrin: a versatile scaffold for tissue engineering applications.* Tissue Engineering Part B: Reviews, 2008. **14**(2): p. 199-215.
43. Schense, J.C. and J.A. Hubbell, *Cross-linking exogenous bifunctional peptides into fibrin gels with factor XIIIa.* Bioconjugate Chemistry, 1999. **10**(1): p. 75-81.
44. Willerth, S.M., et al., *Rationally designed peptides for controlled release of nerve growth factor from fibrin matrices.* Journal of Biomedical Materials Research Part A, 2007. **80A**(1): p. 13-23.
45. Mohtaram, N.K., A. Montgomery, and S.M. Willerth, *Biomaterial-based drug delivery systems for the controlled release of neurotrophic factors.* Biomedical Materials, 2013. **8**(2): p. 022001.
46. Mooney, R., B. Tawil, and M. Mahoney, *Specific fibrinogen and thrombin concentrations promote neuronal rather than glial growth when primary neural cells are seeded within plasma-derived fibrin gels.* Tissue Eng Part A, 2010. **16**(5): p. 1607-19.
47. Dahlstrand, J., M. Lardelli, and U. Lendahl, *Nestin mRNA expression correlates with the central nervous system progenitor cell state in many, but not all, regions of developing central nervous system.* Developmental Brain Research, 1995. **84**(1): p. 109-129.
48. Wegner, M. and C.C. Stolt, *From stem cells to neurons and glia: a Soxist's view of neural development.* Trends in Neurosciences, 2005. **28**(11): p. 583-588.
49. Schwartz, P.H., et al., *Differentiation of neural lineage cells from human pluripotent stem cells.* Methods, 2008. **45**(2): p. 142-158.
50. Wosnick, J.H., M.D. Baumann, and M.S. Shoichet, *73 - Tissue Therapy: Central Nervous System*, in *Principles of Regenerative Medicine*. 2008, Academic Press: San Diego. p. 1248-1269.
51. Karumbayaram, S., et al., *Directed Differentiation of Human-Induced Pluripotent Stem Cells Generates Active Motor Neurons.* Stem Cells, 2009. **27**(4): p. 806-811.
52. Kolemainen, K. and S.M. Willerth, *Preparation of 3D fibrin scaffolds for stem cell culture applications.* Journal of Visualized Experiments, 2012. **61**: p. e3641.